

Corneal nerves segmentation and morphometric parameters quantification for early detection of diabetic neuropathy

Ana Ferreira¹, António Miguel Morgado^{1,2} and José Silvestre Silva^{2,3}

¹ IBILI – Institute of Biomedical Research in Light and Image, Faculty of Medicine, University of Coimbra, Portugal

² Department of Physics, Faculty of Sciences and Technology, University of Coimbra, Portugal

³ Instrumentation Center, Faculty of Sciences and Technology, University of Coimbra, Portugal

Abstract—Morphological parameters of the corneal sub-basal nerve plexus may be the basis of a simple and noninvasive method for detection and follow-up of diabetic neuropathy. These nerves can be analyzed from images obtained *in vivo* by corneal confocal microscopy. In this work we present and evaluate an automatic methodology capable of identifying corneal nerves and determine various morphometric parameters.

Keywords— diabetic neuropathy, corneal nerves, automatic segmentation, corneal confocal microscopy.

I. INTRODUCTION

The cornea is one of the most highly innervated tissues in the human body. It is possible to image *in vivo* the corneal layers and membranes, using corneal confocal microscopy (CCM). In particular, it is possible to image the sub-basal nerve plexus and to document and quantify changes in corneal nerves morphology. There has been an increasing interest in using corneal nerves for early diagnosis and accurate assessment of peripheral neuropathy, a major cause of morbidity in diabetic patients [1, 2], which are important to define the higher risk patients, decrease morbidity and assess new therapies [3].

There are several *in vivo* studies published that quantify nerve density [4], evaluate changes in morphology of sub-basal nerves [5] or elucidate the overall distribution of these nerves [6]. Other studies demonstrated that CCM can accurately define the extent of corneal nerve damage and repair, proving that it can be used as a measure of peripheral neuropathy in diabetic patients [7], allows the evaluation of corneal nerve tortuosity and that this parameter relates to neuropathy severity [8] or compared basal epithelium cell density between patients with diabetic retinopathy and controls to determine whether corneal basal epithelium density is associated with alterations on corneal innervation [9].

Our group has done relevant research on diabetic corneas using CCM, showing that the number of fibers in the sub-basal nerve plexus of patients was significantly lower than in healthy humans, even for short diabetes duration, opening the possibility of using the assessment of corneal innerva-

tion by CCM for early diagnosis of peripheral neuropathy [5], a result later confirmed by other authors [10].

Currently, the corneal nerves analysis is based on a tedious process of manual tracing of the nerves, using confocal microscope built-in software [11], commercial programs [11-14] or software specifically developed for the purpose [14]. The extraction of clinical information is subjective and prone to errors.

Thus, an automatic tool capable of extract and quantify the sub-basal plexus morphometric parameters may be the ideal method to evaluate nerve pathologies in diabetic patients and may constitute a basis for diabetic neuropathy diagnosis [15, 16].

Scarpa et al. [17] proposed automatic methods for the recognition and tracing of the corneal nerve structures. The nerves were recognized by a tracing algorithm based on filtering and pixel classification methods with post-processing to remove false recognitions and link sparse segments into continuous structures. Automatic and manual length estimations on the same image were well correlated.

In the past, we proposed an automatic method capable of identifying straight nerves [18]. When nerves had a curved shape or sudden changes of direction, additional processing was necessary. This way, an entropy-based method was developed with considerably better results [19]. However, the pre-processing step induced noise, resulting in false nerve branches. This prompted further improvements leading to a new algorithm capable of reliable extraction of the nerve structure and to measure morphometric parameters. The development of such a tool is reported in this work.

II. MATERIALS AND METHODS

A. Corneal nerves segmentation

1. Image acquisition

We used corneal nerve images acquired *in vivo*, by researchers at the University of Padova, from diabetic and non-diabetic patients, using a CCM (ConfoScan4, Nidek Technologies, Padova, Italy), with a 460×350 μm field of

view using a 40X objective, and compressed in JPEG monochrome format, with a size of 768×576 pixels. These images are available online [17].

2. Image Pre-Processing

In a CCM image, the background is often characterized by a gradual intensity variation from the periphery to the center, with the central region being brighter. Nerves stand out from the background and normally appear as bright linear structures over a dark background. For correcting this non-uniformity of contrast, it is necessary to apply a pre-processing method to the images, before segmentation.

We applied local equalization to the original images, based on the histogram of a region with size of 8×8 pixels, to increase the contrast.

In order to enhance the boundaries of structures in the image, a phase symmetry algorithm, based on local frequency information analysis, was used. This overcome the need to segment the objects first and not providing any absolute measure of the degree of symmetry at any point in the image [13].

Finally, we investigated the histogram of the image, applying the highest dynamic threshold, in such a way that at least 10% of the image pixels are above that threshold. Thus, some noise is removed and in some way and edges that correspond to nerves are identified, as the number of pixels of the nerves is usually less than 10% of the total pixels of the image.

3. Nerves reconstruction

The recognition of the nerves involves several steps, but is mainly based on the region growth approach. It starts with two region growth applications to the binary image: one from all the pixels that are 5% distant from the margin and other from pixels 35% away from the image border.

A comparison between those regions that have grown (nerves) and those regions that have not grown (noise) is made, removing the noise.

Then, several morphological operations are applied. The morphologic skeleton of the image is computed and branches with less than 10 pixels (spurious branches) are removed. After that, each disconnected region on the image is identified: those isolated and with small area are discarded, as they are regions with a lot of consistent noise or small nerves which do not represent continuous structures.

The resultant nerves are compared with the original image just after the threshold and their endpoints are grown along the major axis to reconstruct the nerves to their original dimensions.

B. Morphometric parameters calculation

1. Length

The lengths (μm) of the nerve structures were calculated by simply computing the size of the nerve skeleton.

2. Tortuosity Coefficient

The Tortuosity Coefficient (TC) is a parameter that gives information on the frequency and magnitude of nerve curvature changes. To calculate it we consider each nerve as a mathematical function on the image space and compute the function first and second derivatives [8].

In order to treat each nerve as a mathematical function, we find its endpoints, draw a straight line between them and rotate the image, aligning the straight line with the x-axis.

The TC is calculated by:

$$TC = \sqrt{\sum_{i=1}^{N-1} ((f'(x_i, y_i))^2 + (f''(x_i, y_i))^2)} \quad (1)$$

With N the number of pixels of the nerve skeleton, $f'(x_i, y_i)$ and $f''(x_i, y_i)$ are the first and second derivatives at the point (x_i, y_i) , respectively.

C. Performance evaluation

The automatic algorithm was evaluated against manual segmentation of the corneal nerves by an experienced ophthalmologist. Pixel classification (nerve or non-nerve) was compared between automatically and manually segmented images. The nerve length correctly recognized by the algorithm and the nerve length traced by manually tools, were compared. The manual nerve segmentation and length measurement was accomplished with the help of the Simple Neurite Tracer plug-in for Fiji [20].

III. RESULTS AND DISCUSSION

Fifteen (15) corneal nerves images were tested using the proposed methods. Fig.1 shows a representative example of the results obtained with the corneal nerves segmentation algorithm. To evaluate the performance of the method we compared the nerve length correctly recognized by the algorithm, with the length of manually traced nerves on the same image.

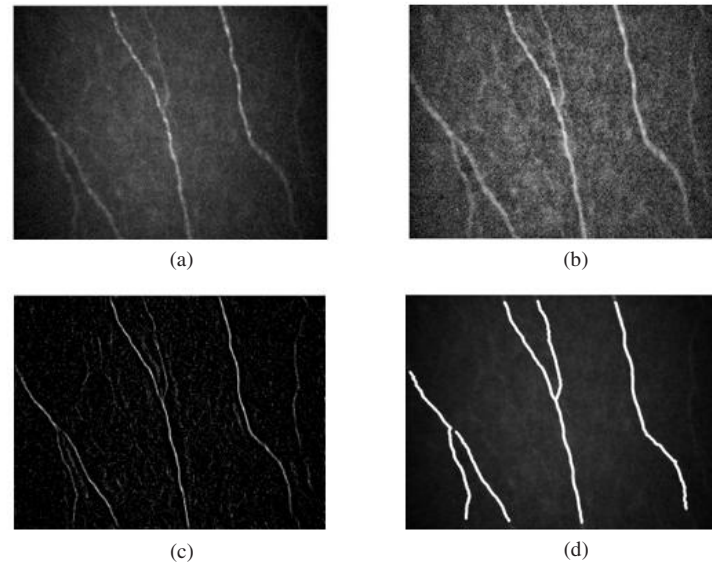


Fig. 1 Representative example of the corneal nerves segmentation method: (a) original image, (b) normalized image, (c) after phase shift, (d) segmented image.

The average percent of nerve correctly segmented by the algorithm was $87.1\% \pm 8.1\%$ (range: 73.5% - 96.8%). No image structures were falsely reported as nerves by the algorithm although there are pixels falsely classified as nerves (when compared with manual segmentation) due to differences on the nerve widths. Fig. 2 shows a Bland and Altman plot [21] for the comparison between automatic and manual nerve length measurement. The average difference between nerve lengths was $-38.0 \pm 45.8 \mu\text{m}$. This means that, in 95% of the cases, the difference between nerve lengths measured automatically and manually will lie between -127.7 and $51.7 \mu\text{m}$. These limits, as well as the average difference, are shown in the plot. These results are similar to those reported in the literature and also show underestimation by the automatic method [17].

In the segmentation process every image pixel is classified either as nerve or non-nerve. By comparing the outcome of the automatic segmentation with the manual segmentation results, which are taken as the standard, it is possible to classify every image pixel according to four events: true positive (TP) and true negative (TN), when a pixel is classified in the same way by the automatic and manual segmentation processes, a false negative (FN) when a pixel classified as nerve by the manual process is segmented as non-nerve by the automatic algorithm and a false positive (FP) when a non-nerve pixel is segmented as a nerve by the automatic algorithm.

From these events it is possible to calculate the sensitivity and specificity of the automatic segmentation algorithm.

The sensitivity measures the proportion of true positives, while specificity measures the proportion of true negatives:

$$\text{sensitivity} = \frac{TP}{TP+FN} \quad \text{specificity} = \frac{TN}{TN+FP} \quad (2)$$

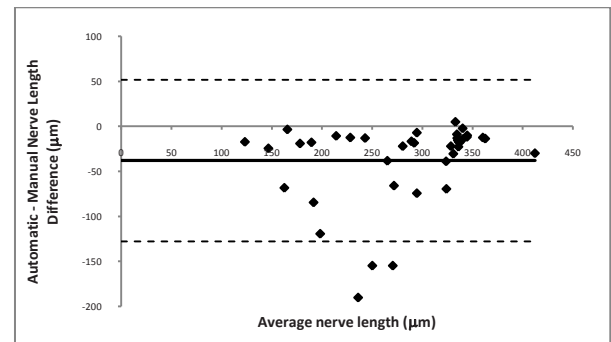


Fig. 2 Comparison of nerve length measurement between automatic and manual segmentation.

There is a tradeoff between these two figures. Our option was to minimize the false positive rate since we considered that is more important to prevent the identification of false nerves than to identify correctly all the nerve length as nerve morphometric parameters, like the Tortuosity Coefficient can be successfully extracted from nerve segments.

The false positive rate (FPR) is defined according to:

$$\text{FPR} = \frac{FP}{FP+TN} = 1 - \text{specificity} \quad (3)$$

The accuracy of the segmentation is defined by

$$\text{accuracy} = \frac{TP+TN}{P+N} \quad (4)$$

where P and N are the total number of positives and negatives pixels in the segmentation process.

For the set of 15 segmented images, the average sensitivity was $66.6\% \pm 10.4\%$ (range: 48.3% - 77.7%). This value results not only from nerve segments that were not identified as such by the automatic segmentation but mainly from differences in the nerves width between manual and automatic segmentation.

The average specificity was $99.6\% \pm 0.2\%$ (range: 99.3% - 99.9%), which is equivalent to a FPR of 0.4%. This shows that no corneal structures were falsely classified as nerves. The average accuracy of the automatic segmentation was $98.6\% \pm 0.5\%$ (range: 97.9% - 99.2%).

From the nerves representation obtained through automatic segmentation we have extracted the TC morphometric parameter. The average value of the TC was 26.8 ± 10.5 (range: 15.3 - 33.3). This value agrees with those previously reported, using the same definition of tortuosity, for non-diabetic and mild-neuropathy diabetic individuals [8].

The proposed algorithm for nerve identification was fully automatic, requiring no user intervention. Running times were around 3 minutes on an Intel® Centrino Core™2 Duo at 2.4 GHz computer.

In conclusion, the developed algorithm produced good results, in terms of nerves detected and nerve length measurement, while providing an excellent specificity. It yields Tortuosity Coefficients in agreement to those found in the literature. The issues related to non-uniform contrast and luminosity were successfully solved by pre-processing the images with local equalization and phase shift based methods. There is still room for improvement particularly when dealing with images containing nerve branches.

In our opinion, the need for a simple, non-invasive technique, capable of accurately documenting the extent of nerve damage and repair, for early diagnosis of peripheral diabetic neuropathy, can be addressed through the evaluation of corneal nerve morphology, using CCM images. In this work we presented an automatic algorithm for analysis of corneal sub-basal nerve plexus images. This work is part of a broader project that aims to develop a noninvasive technique for early diagnosis and monitoring of diabetic neuropathy.

REFERENCES

1. Gooch Clifton et al. (2004) The Diabetic Neuropathies. *The Neurologist*, vol. 10, pp. 311-322

2. Hossain Parwez, Sachdev Arun et al. (2005) Early detection of diabetic peripheral neuropathy with corneal confocal microscopy. *The Lancet*, vol. 366, pp. 1340-1343
3. T. S. Park, J. H. Park et al. (2004) Can diabetic neuropathy be prevented? *Diabetes research and clinical practice*, vol. 66, pp. S53-S56
4. Grupcheva C. N., Wong T. et al. (2002) Assessing the sub-basal nerve plexus of the living healthy human cornea by in vivo confocal microscopy. *Clinical and Experimental Ophthalmology*, vol. 30, pp. 187-190
5. Popper, M., Quadrado, M.J., Morgado, A.M., Murta, J.N., Van Best, J.A., Muller, L.J. (2005) Subbasal Nerves and Highly Reflective Cells in Corneas of Diabetic Patients: In vivo Evaluation by Confocal Microscopy. *Invest. Ophthalmol. Vis. Sci.*, vol. 46
6. Patel, D.V., McGhee et al. (2005) Mapping of the Normal Human Corneal Sub-Basal Nerve Plexus by In Vivo Laser Scanning Confocal Microscopy. *Invest. Ophthalmol. Vis. Sci.*, vol. 46, pp. 4485-4488
7. Malik, R.A., Kallinikos, P., Abbott, C.A., van Schie, C.H.M., Morgan, P., Efron, N., Boulton et al. (2003) Corneal confocal microscopy: a non-invasive surrogate of nerve fibre damage and repair in diabetic patients. *Diabetologia*, vol. 46, pp. 683-688
8. Kallinikos Panagiotis, Berhanu Michael, O'Donnell Clare, Boulton Andrew J. M., Efron Nathan et al. (2004) Corneal Nerve Tortuosity in Diabetic Patients with Neuropathy. *Invest. Ophthalmol. Vis. Sci.*, vol. 45, pp. 418-422
9. Chang P. Y., Carrel H., Huang J. S., Wang I. J., Hou Y. C., Chen W. L., Wang J. Y. et al (2006) Decreased density of corneal basal epithelium and subbasal corneal nerve bundle changes in patients with diabetic retinopathy. *American journal of ophthalmology*, vol. 142, pp. 488-490
10. Midena E., Brugin E., Ghirlando A., Somavilla M. et al. (2006) Corneal diabetic neuropathy: A confocal microscopy study. *Journal of Refractive Surgery*, vol. 22, pp. S1047-S1052
11. Frangi A.F., Niessen W.J., Vincken K.L., Viergever M.A. (1998) Multiscale vessel enhancement filtering. *Medical Image Computing and Computer-Assisted Intervention - Miccai'98*, vol. 1496, pp. 130-137
12. McLaren J.W., Nau C.B., Kitzmann A.S., Bourne W.M. (2004) Keratocyte Density: Comparison Of Two Confocal Microscopes. *Invest. Ophthalmol. Vis. Sci.*, vol. 45
13. Kovesi P. (1997) Symmetry and Asymmetry from local phase. Tenth Australian Joint Conference on Artificial intelligence, vol.
14. Bilgin C., Bullough P., Plopper G., Yener B. ECM-aware cell-graph mining for bone tissue modeling and classification. *Data Mining and Knowledge Discovery*
15. Stachs O., Zhivov A., Kraak R., Stave J., Guthoff, R. (2007) In vivo three-dimensional confocal laser scanning microscopy of the epithelial nerve structure in the human cornea. *Graefes Archive for Clinical and Experimental Ophthalmology*, vol. 245, pp. 569-575
16. Mocan M. C., Durukan I., Irkec M., M., O. (2006) Morphologic alterations of both the stromal and subbasal nerves in the corneas of patients with diabetes. *Cornea*, vol. 25, pp. 769-773
17. Scarpa F., Grisan E. et al. (2008) Automatic Recognition of Corneal Nerve Structures in Images from Confocal Microscopy. *Investigative Ophthalmology & Visual Science*, vol. 49, pp. 4801-4807
18. Silva J.S., Morgado A.M. (2008) Caracterização dos Nervos da Córnea para o Diagnóstico de Diabetes. *RecPad (Conferência Portuguesa de Reconhecimento de Padrões)*
19. Ana Ferreira, António Miguel Morgado, Silva J.S. (2009) Corneal nerves identification for earlier diagnosis and follow-up of diabetes. *RecPad (Conferência Portuguesa de Reconhecimento de Padrões)*
20. <http://homepages.inf.ed.ac.uk/s9808248/imagej/tracer/>
21. Bland J.M., Altman D.G. (1986) Statistical methods for assessing agreement between two methods of clinical measurement. *Lancet*, vol. 1, pp. 307-310.